ELSEVIER

Journal of Power Sources 52 (1994) 61–68

JOURNAL OF POWER SOURCES

Overcharge in the vanadium redox battery and changes in electrical resistivity and surface functionality of graphite-felt electrodes

F. Mohammadi[a], P. Timbrell[b], S. Zhong[a], C. Padeste[a], M. Skyllas-Kazacos[a,*]

[a]*School of Chemical Engineering and Industrial Chemistry, University of New South Wales, P O Box 1, Kensington, NSW 2033, Australia*

[b]*Surface Science and Technology, School of Chemistry, University of New South Wales, P O. Box 1, Kensington, NSW 2033, Australia*

Received 2 February, 1994; accepted 25 April, 1994

Abstract

The influence of overcharge on the performance of the vanadium redox cell that employs graphite-felt electrodes is examined. The electrical, electrochemical and surface properties of the graphite-felt electrodes are investigated in order to determine the contribution and effect of each deterioration mechanism to the loss in cell performance during overcharge. The electrical resistivity of the electrodes and the cell resistance show a slight increase after overcharge. The effect of overcharge on the surface chemistry of three types of graphite-felt electrodes is investigated using X-ray photoelectron spectroscopy (XPS). The XPS analysis reveal a slight increase in the overall surface oxygen content of the graphite felts after overcharge, together with a shift to higher oxidation states that is consistant with the formation of C–OH, –C=O, –COOH and –COOR groups. The proportion of each of these groups varies between graphite-felt types. The measured change in the relative concentrations of surface oxygen functional groups on the graphite felt is believed to be responsible for the observed increase in the electrical resistivity and electrochemical activity of the electrode materials during cell overcharge.

Keywords Vanadium redox batteries; Electrical resistivity; Electrodes, Graphite felt

1. Introduction

Carbon or graphite felts are widely used as electrode active layers in carbon–plastic composite electrodes for redox flow-cell applications [1–7]. Depending on the precursors, processing conditions, forming methods, and other parameters such as heating rate and final temperature, the final characteristics of the felts vary considerably [8–11]. These differences are attributed to the surface microstructure and defect concentration of the fibres of the felts which affect the extent of carbon–oxygen interaction. This is of great importance for electrode materials, since it will result in different behaviour towards the formation of carbon–oxygen surface functional groups, which links directly to the electroactivity and oxidation stability of the graphite-felt electrodes [5–7].

The vanadium redox flow cell employs V(II)/V(III) and V(IV)/V(V) couples in the negative and positive half-cell electrolytes, respectively, with H_2SO_4 as the supporting electrolyte and graphite felt as the electrode material. Under overcharge conditions, O_2 and CO_2 evolution can occur at the anode while H_2 evolution takes place at the cathode.

In a previous paper [12], we reported a comparison of two typical graphite felts that are currently used as electrodes in prototype vanadium redox batteries. Some differences were found in the physical, chemical and electrochemical properties of rayon and polyacrylonitrile (PAN)-based graphite-felt materials. In the present paper, the overcharge behaviour of three types of graphite-felt electrodes in the positive half-cell of the vanadium redox battery is presented, and the effect of overcharge on the formation of carbon–oxygen surface functional groups on the felt electrodes is reported. The oxidation behaviour of the three typical graphite felts operated in a vanadium redox cell under normal cell operation and overcharge conditions has been studied by cyclic voltammetry, electrical resistivity measurements and X-ray photoelectron spectroscopy (XPS). Graphite felts, based on rayon and PAN, were anodically oxidized at a positive electrode potential to compare the effect of anodic oxidation on the electrochemical response of the felt in sulfuric acid solution. Gas

*Corresponding author.

0378-7753/94/$07 00 © 1994 Elsevier Science S A. All rights reserved
SSDI 0378-7753(94)01938-R

oxidation experiments were also performed on these felt samples.

2. Experimental

The graphite felts were fabricated into rectangular electrodes and subjected to various overcharge conditions within a single redox flow cell. The electrical and electrochemical properties, as well as the surface chemistry of these felt materials, were characterized before and after overcharge.

2.1. Graphite-felt materials

The following three types of felt materials were examined:
(i) Sigri GFD2 graphite felt, approximately 2.8 mm thickness, PAN-based (Sigri Electrographite GmbH, Germany);
(ii) Sigri GFD5 graphite felt, approximately 5.9 mm thickness, PAN-based (Sigri Electrographite GmbH, Germany), and
(iii) FMI graphite felt, approximately 6 mm thickness, rayon-based (Fibre Materials Inc., Maine, USA).

2.2. Electrical resistivity

The volume resistivities of various felt materials were measured, before and after overcharge, according to the ASTM-D991.

2.3. Test cell

A modified NASA-design cavity fill-in redox flow cell [13] was employed for the overcharge studies. The expanded diagram of a laboratory-scale cell used for evaluating the overcharge behaviour of the graphite-felt electrodes is shown in Fig. 1. The components of each half-cell consist of an end-electrode, separator, flow frame, current collector, insulating plate and end-plate. The projected area of the electrodes was 138 cm^2. The graphite felt was compressed against a graphite-plate current collector. In the case of the GFD2 sample, two sheets were inserted to obtain adequate compression and electrical contact with the current collector. A cation-exchange membrane (Selemion CMV-Asahi Glass Co., Japan) was employed as the separator, while a window-cut poly(vinyl chloride) (PVC) plate with solution outlet and inlet was served as a flow frame. Two copper plates, identical in size to the electrodes, acted as current collectors. Before the aluminium end-plate, a PVC plate was employed as an insulating layer to prevent the two halves of the cell from short-circuiting. Both half-cells had the same components and configuration and were assembled by bolts and nuts between two end-plates.

Equal volumes of 1 M V(IV) in 2.5 M H_2SO_4 solution were used initially in each half-cell to generate the V(V) positive and V(II) negative fully charged electrolytes from an initial charging cycle.

2.4. Cell resistance

The electrochemical properties of the felt-electrode-based cells were determined by measuring the cell resistance, R_{cell} (Ω cm^2), which is a criterion for evaluation of the entire system resistance. This term reflects any changes in the electronic or ionic resistance of a cell/battery due to changes in the characteristics of the electrodes, electrolyte and/or membrane. Values of cell resistance were obtained from plots of cell current versus cell voltage obtained at 50% SOC during both charge and discharge of a vanadium redox cell [12].

2.5. Overcharge of felt electrodes

One or two pieces of felt (6 cm × 5 cm), with measured electrical resistivity, were placed between the graphite current collector and the membrane in each half-cell of the flow cell, shown in Fig. 1. Cell resistance measurements were carried out at 50% state-of-charge (SOC) before any treatment, and then the cell was fully charged to 100% SOC. An overcharge condition was applied to the cell by passing a current of 21.7 mA cm^{-2} through the fully charged cell for either 50 min or 3 h. To characterize the effect of overcharge on the graphite felt alone, the cell was then pulled apart and the positive graphite-plate current collector was polished with 1200 μm sandpaper and washed with distilled water until an even, clean and conductive surface was achieved. The cell was then reassembled and the cell resistance at 50% SOC was measured. The cell was again disassembled and the felt electrodes removed from the cell, washed an immersed in distilled water for three days. The felt samples were dried in air and their volume resistivity redetermined.

2.6. Preparation of graphite-felt samples for XPS analysis

The overcharged positive electrodes were removed from the cell, washed thoroughly with tap water, and then immersed in distilled water overnight. After draining the water from the felts, the cleaned electrodes were dried either in air or in an oven at 60 °C for 8 h. For comparison, FMI and GFD2 felt samples were also taken from the positive electrodes operated for 25 cycles (100 h) in a vanadium redox battery under normal charging/discharging conditions, i.e., in the potential range of 0.8 to 1.7 V where the vanadium redox reactions are predominant (named as 'AC'). These

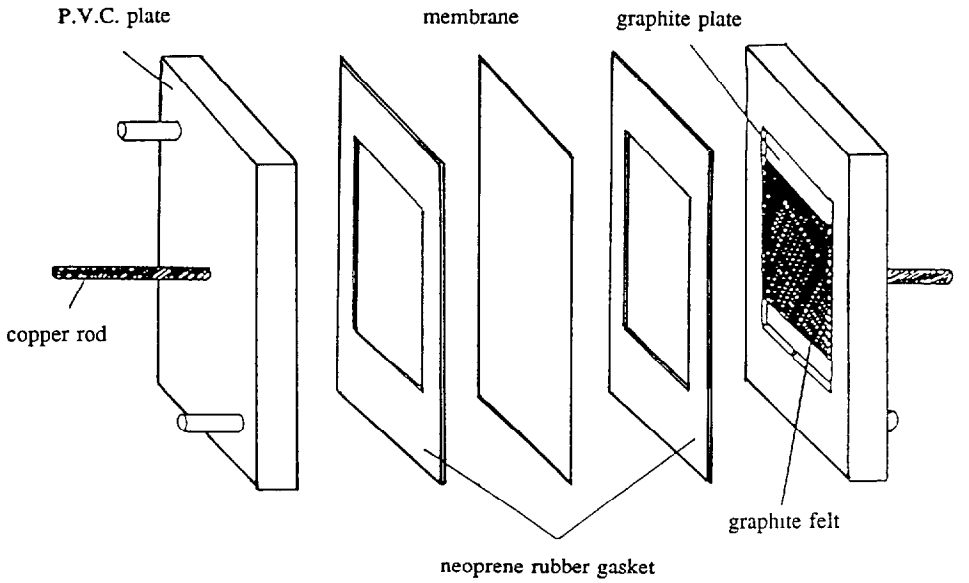

Fig. 1. Expanded diagram of a single cell vanadium redox flow battery used for overcharge study of graphite-felt electrodes

samples were cleaned in the same way and dried in an oven at 60 °C for 8 h.

2.7. X-ray photoelectron spectroscopy (XPS)

The felt electrode samples were cut into 15 mm diameter discs and fixed on to the sample stub with double-sided tape for the XPS analysis. The XPS spectra were collected on a KRATOS XSAM 800 spectrometer (hemispherical analyser) using unmonochromated Mg Kα radiation at 180 W power. The spectrometer binding energy scale was calibrated to the Cu $2p_{3/2}$ line ($E_B = 932.7$ eV) and Ag $3d_{5/2}$ ($E_B = 386.2$ eV) line. The spectrometer was run in the FAT (fixed angular transmission) mode. The analyser pass energy was set at 160 eV (1 eV step size) for the wide scans and elemental analysis, and at 40 eV (0.1 eV step size), to yield an instrumental resolution of approximately 1.1 eV, for the detailed C 1s and O 1s lineshape analysis. Mixed 50/50 lorentzian-gaussian lineshapes and non-linear Shirley background subtraction were used for the O 1s and C 1s curve fitting.

2.8. Cyclic voltammetry

The supporting electrolyte of the vanadium redox flow cell, 3 M H_2SO_4, was used for anodic oxidation experiments on the PAN and rayon graphite-felt electrodes. Cyclic voltammograms were recorded before and after anodic oxidation. The latter was performed by holding the electrodes at a positive potential of +1.5 V versus a Hg/Hg_2SO_4 reference electrode for 15 min. In order to avoid an accumulation of gas bubbles inside the felt, the electrode was rotated at a speed of 500 rpm during the anodic oxidation.

3. Results and discussion

3.1. Effect of overcharge on electrical resistivity

Table 1 shows the effect of overcharge on the electrical resistivity of various felt materials overcharged in 2 M VO_2^+/3 M H_2SO_4 solution (catholyte) at 21.7 mA cm^{-2} for 50 and 180 min. As is obvious from these results, for both the rayon (FMI) and PAN-based (GFD) graphite-felt electrodes, the volume resistivity of the positive felt electrode increased slightly after overcharge. The effect of the net overcharge time in the range studied (up to 3 h) is not significant. From comparison of the resistivity values of each Sigri positive felt electrode overcharged for 180 min with those obtained for 50 min overcharge, a slight increase can be seen. The results obtained for the FMI sample do not follow this trend. The FMI sample overcharged for 180 min was, however, from a different batch which may possibly have been more graphitized and thus less susceptible to interaction with oxygen compared with the FMI sample overcharged for 50 min. The electrical resistivity of the negative felt electrodes was also measured and it was found that even at the severe overcharge condition of 3 h, the change in electrical resistivity was less than 0.014 Ω cm^2.

3.2. Effect of overcharge on cell resistance

A series of resistance measurements of a cell that employed various felt electrodes was performed before and after overcharge to characterize the effect of overcharge on cell performance.

Table 2 shows the values of resistance for a cell with either untreated electrodes or electrodes that had been

Table 1
Effect of overcharge on electrical resistivity of graphite-felt materials, anodically overcharged in 2 M VO_2^+/2 M H_2SO_4 at 21.7 mA cm^{-2}

Felt electrode	Overcharge time (min)	$\rho_{untreat}$ (Ω cm)	$\rho_{overcharge}$ (Ω cm)	$\Delta\rho$ (Ω cm)	$\Delta\rho\ d_{pos}$ (Ω cm^2)
FMI	50	0.1692	0 5721	0.4029	0 24
FMI	180	0.1523	0 4002	0.2479	0 13
Sigri GFD5	50	0 1417	0.3314	0.1819	0 11
Sigri GFD5	180	0.1340	0.4890	0.3550	0 21
Sigri GFD2	50	0 1003	0.2380	0.1377	0 038
Sigri GFD2	180	0.1087	0.2471	0.1384	0 039

Table 2
Cell resistance after overcharge with 2 M $VOSO_4$/3 M H_2SO_4 at 21.7 mA cm^{-2}

Felt electrode	Overcharge time (min)	Untreated R_{cell} (Ω cm^2)	Overcharge R_{cell} (Ω cm^2)	ΔR_{cell} (Ω cm^2)
FMI	50	4.19	4 84	0 65
FMI	180	4.97	5 40	0 43
Sigri GFD5	50	3.67	4 86	1 19
Sigri GFD5	180	4.61	5 96	1 35
Sigri GFD2	50	7.61	7.78	0 17
Sigri GFD2	180	7.35	8.53	1 18

overcharged in 2 M VO_2^+/3 M H_2SO_4 at 21.7 mA cm^{-2} for 50 and 180 min with subsequent polishing of the graphite-plate current-collector. The difference in cell resistance that is due solely to oxidation of the felt is also summarized. For both rayon and PAN-based graphite felts, a slight increase in the cell resistance after overcharge is observed. The highest increase in cell resistance with overcharge corresponds to the GFD5 electrode which showed an increase from 4.61 to 5.96 Ω cm^2 after 3 h overcharge. For the GFD2 felt, a slightly higher resistance was measured and this is attributed to the poorer contact between the GFD2 felt with the graphite current collector that is caused by the lower compression of the thinner felt sample in the cell cavity. Again, the FMI sample used for the 180 min test was from a different bath than that overcharged for 50 min, so direct comparison cannot be made. These results for the FMI felt do, however, highlight the great variability in properties of graphite-felt materials from different batches from the same manufacturer.

3.3 XPS analysis

The surface elemental composition, as well as the changes in surface functionality, of the felt electrodes due to overcharge were characterized using XPS analysis. The overcharged graphite-felt samples were prepared as explained earlier, and their surface chemistry compared with that of untreated and thermally-treated samples in N_2 at 400 °C for 30 h.

3.4. General spectra

Fig. 2 illustrates a typical XPS wide-scan spectrum obtained from graphite-felt electrodes, along with the spectrum obtained from a GDF5 sample overcharged for 50 min (OC1). In all cases, strong C 1s and O 1s photoelectron lines are observed at $E_B = 285$ and 533 eV, respectively. Weaker O(KLL) and C(KLL) Auger features are in evidence at approximately 760 and 1000 eV. In general, the O 1s line is seen to increase in intensity with overcharging (increasing oxidation) and

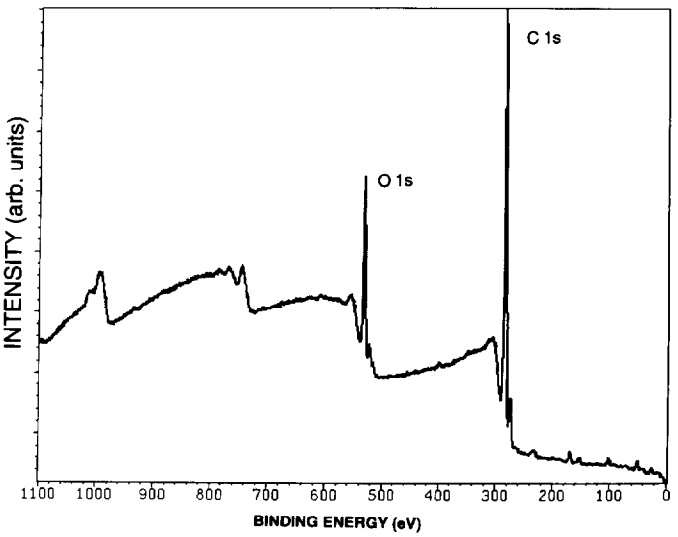

Fig 2 Typical wide-scan X-ray photoelectron spectroscopy spectrum obtained from a graphite-felt electrode sample (GDF5 sample shown here). The main O 1s and C 1s peaks are indicated.

the general spectra for graphite felts have been reported earlier [12,13]. High-resolution scans of the C 1s and O 1s regions are presented here. Table 3 summarizes the measured surface O and C elemental composition (atomic percentages) for the various felt-electrode samples (GFD5, GFD2 and FMI) exposed to different treatments abbreviated as UNT, AIR, AC, OC1 and OC2.

The increase in the atomic oxygen concentration of the GFD5 felt after various treatments is shown in Table 3. The overall oxygen content of the samples increases with increasing severity of oxidation. Comparison of the N2T and OC2 samples shows a slight increase in the O/C ratio from 0.177 to 0.217 for the positive electrode sample that has been overcharged for 3 h in the test cell (OC2).

Comparing the oxygen concentration of the N2T-treated GFD5, GFD2 and FMI samples in Table 3, a considerable difference between samples is observed. In each case, the oxygen concentration is seen to increase in the overcharged samples. The effect of normal cell operation on the oxygen concentration is also given in Table 3 for the GFD2 and FMI felt samples, and an increase in the O/C ratio is again observed, although this is not as great as for the overcharged samples.

3.5. O 1s and C 1s spectra

The high-resolution spectra of the O 1s and C 1s peaks were obtained to determine oxygen functionality of the felts both before and after overcharge. Figs. 3 (a) to (c) present the curve-fitted O 1s and C 1s spectra of samples N2T, OC1 and OC2 for the GFD5 felt. The spectra have been fitted to various C–O functional groups that are known to be found on carbon/graphite surfaces, mainly based on the peak assignment of Sherwood and co-workers [14–23]. The main carbon peak at the lowest binding energy lies in the range at 283.6 to 284.6 eV. The four types of oxide (labelled oxide 1, 2, 3 and 4) were fitted to component peaks shifted by 1.5, 3.1, 4.5 and 6.0 eV from the main peak, respectively. Oxide 1 corresponds to carbon atoms in hydroxide (C–OH) or ether (C–O–C) groups, and oxide 2 is assigned to carbon atoms in carbonyl (C=O) type groups. Oxide 3 is the peak corresponding to ether carboxyl (COOH) or ester (COOR) types of groups. Oxide 4 is attributed to the π–π^* shake-up satellite that serves as an indicator of the degree of aromaticity (graphitization) of the surface, as well as $-CO_3^-$-type groups. The O 1s region was fitted with a two-component curve fit. The main lower binding energy peak (E_B about 532 eV) is attributed to carbonyl (C=O) and ether (C–O–C) oxygen functionalities, while the higher binding energy component, shifted by 1.5 eV is attributed to hydroxyl (–OH) groups.

The peak position and peak area percentage for the C 1s and O 1s spectra are given in Tables 4 and 5, respectively. Although the change in the graphitic peak area is not significant for the OC1 samples, a more pronounced decrease in this peak area is seen for the OC2 sample. In oxide 4, C 1s peak decreases in intensity with overcharging, and is very weak in the OC2 sample, which strongly suggests that a $\pi \rightarrow \pi^*$ shake-up resonance is lost when the aromaticity of the graphite felt is destroyed through the oxidation process. It can also be seen that overcharge results in an increase in the oxide 1 peak area, and that with increased overcharge time the corresponding amount of –OH groups increases. The highest peak area corresponding to oxide 2 and oxide 3 is exhibited by samples OC2. This indicates that with prolonged overcharging there is an overall shift to surface functional groups of higher oxidation state (e.g., C=O).

Operation under severe oxidation conditions of overcharge thus results in oxidation of the graphite felt by the formation of various C–O functional groups, particularly –OH groups (oxide 1). These findings also show that the $-CO_3^-$-type groups constitute only about 1% of the total oxide produced on the surface of the GFD5 felt electrode, even after 3 h of overcharge. It can thus be concluded that the formation of this functional group on the surface of a felt electrode should not be a major contributor to any serious changes in the electrical and electrochemical properties of the electrode. Nevertheless, the opening of the phenyl rings upon oxidation is evidenced by the loss of the $\pi \rightarrow \pi^*$

Table 3
Atomic concentration of O and C in graphite-felt samples with the indicated treatments The oxygen-to-carbon ratios are also shown (O/C)

Sample identification	Treatment condition	GFD5			GFD2			FMI		
		% O	% C	O/C	% O	% C	O/C	% O	% C	O/C
UNT	Untreated	16.19	83.87	0 187						
AIR	Air, 400 °C, 30 h				2 8	97 2	0.288	7 4	92.6	0 800
N2T	N_2, 400 °C, 30 h	15 02	84.98	0.177	2 2	97 8	0 225	4 0	96 0	0 417
AC	After 25 cycles in vanadium cell				18.3	81 7	0 244	23 0	77.0	0 29
OC1	Overcharged, 50 min	16.44	83.56	0.197	28.3	71 7	0 394	29 3	70.7	0.414
OC2	Overcharged, 3 h	17.84	82.16	0.217						

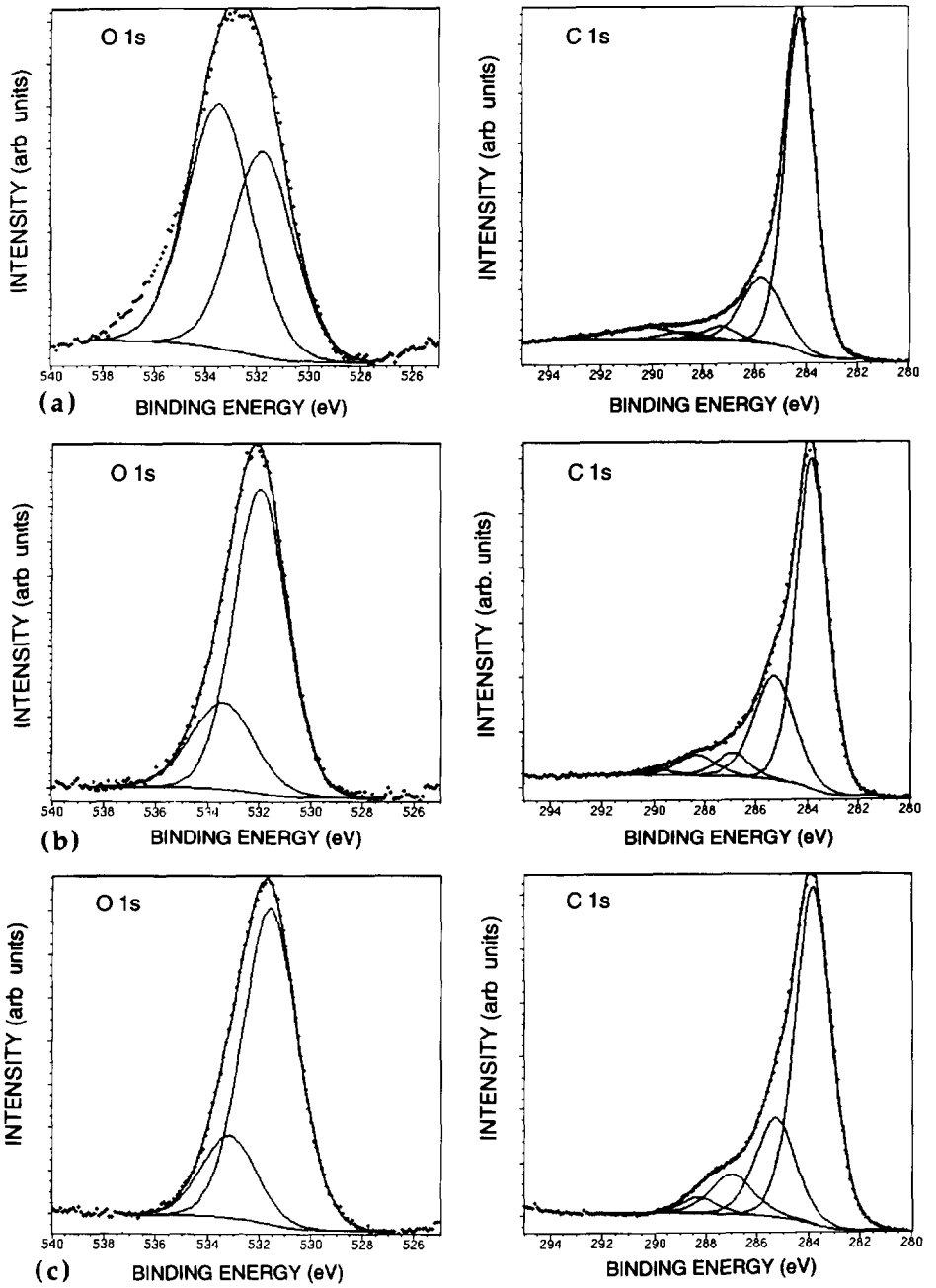

Fig 3 O 1s and C 1s spectra of GFD5 sample: (a) thermally treated in N_2 at 400 °C for 30 h (N2T); (b) after overcharge for 50 min at 21.7 mA cm^{-2} (OC1), and (c) after overcharge for 3 h at 21.7 mA cm^{-2} (OC2). The O 1s and C 1s component peaks are shown and their values given in Tables 4 and 5.

Table 4
C 1s component peak positions (binding energies in eV) and relative concentrations (peak areas) for GDF5 sample

Sample identification	Main peak		Oxide 1		Oxide 2		Oxide 3		Oxide 4	
	Position (eV)	Area (%)	Position (eV)	Area (%)	Position (eV)	Area (%)	Position (eV)	Area (%)	Position (eV)	Area (%)
GFD5, N2T	284 3	70 3	285.8	18.7	287.4	3.2	288.8	2.3	290.3	5.8
GFD5, OC1	283.6	68.8	285.1	24.1	286.8	4.5	288.1	2.2	289.5	3 1
GFD5, OC2	283.8	66.4	285.3	21.2	287	9.4	288 3	3.0	289.8	0 04

Table 5
O 1s component peak positions (binding energies in eV) and relative concentrations (peak areas) for GDF5 sample

Sample identification	Peak 1		Peak 2	
	Position (eV)	Area (%)	Position (eV)	Area (%)
N2T	531.8	43 8	533 5	56 2
OC1	531.7	74.1	533 2	25 9
OC2	531.6	79 6	533.2	20.4

resonance ('oxide 4') which indicates that the surface loses its graphitic character upon overcharge.

The peak position and peak area percentage for the C 1s spectra of the GFD2 and FMI felt samples are given in Table 6 for overcharged samples (OC1) and for samples that have been cycled normally (25 cycles) in a vanadium redox cell (AC). A large decrease in the graphite peak area is observed for the overcharge samples, compared with those subjected to normal cycling. For all samples, the C–OH group (oxide 1) is the predominant species, although the concentration of C–OH groups is slightly higher after overcharge. In the case of oxides 2 and 3, however, a large difference is observed between the AC and OC1 samples. This indicates that, under overcharge conditions, the concentration of the higher oxides C=O, COOH and COOR is increased significantly for both types of felts; the effect is greatest with GFD2 felt.

3.6. Cyclic voltammetry

Fig. 4 shows cyclic voltammograms of the FMI and GFD2 felt electrodes in 3 M H_2SO_4. The potential range was from −1.6 V to +2.50 V. In Fig. 4(a) and (b), curves 1 and 2 refer to the voltammograms obtained before and after anodic oxidation, respectively. Similar cyclic voltammograms for both FMI and GFD2 felt electrodes were observed before anodic oxidation. In addition to the hydrogen and oxygen evolution, a reduction peak around −0.5 V (peak B in Fig. 4(a) and (b)) appears. This indicates that some carbon–oxygen functional groups exist and are reduced at that potential. The results of the XPS analysis presented above suggest that these peaks are predominantly associated with the C–OH groups on the carbon surface. After anodic oxidation, a more clear oxidation peak around +1.3 V (peak A in both cases) is observed. This demonstrates that the concentration of these surface carbon–oxygen functional groups increases at the electrode surface. For the GFD2 felt electrode, an extra reduction peak, peak C, appears at the electrode potential of −1.10 V. This is due to the presence of increased levels of oxides (C=O, COOH and/or COOR) on the surface. These results are consistent with the XPS analysis of

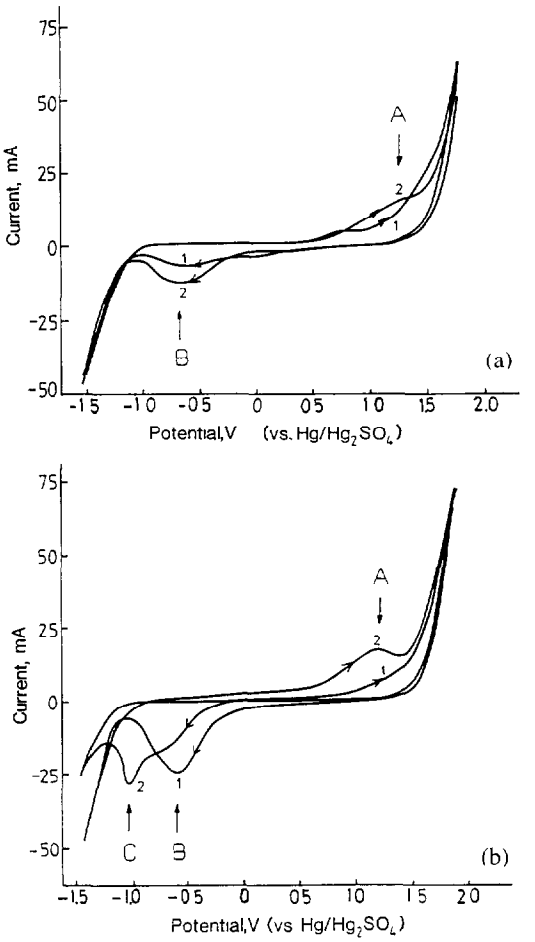

Fig. 4. Cyclic voltamograms for graphite-felt electrodes in 3 M H_2SO_4 solution (1) before anodic oxidation; (2) after holding at +1.5 V for 15 min; (a) FMI, and (b) GFD2. Sweep rate: 60 mV s^{-1}.

Table 5 which showed a greater tendency for the PAN-based GFD2 felt to form the higher oxides under overcharge conditions (e.g., oxide 2 increased by a factor of more than 5 for the GFD2 compared with a factor of 3 for the FMI felt).

4. Conclusions

The electrical resistivity of the positive graphite-felt electrode increased slightly after overcharge with the contribution of less than 0.45 Ω cm^2 to the cell resistance in the case of the GFD5 felt. The increase in cell resistance due to severe electrochemical oxidation of the same felt electrode during overcharge was as high as 1.35 Ω cm^2, however, and suggested that a slight loss in electrochemical activity of the felt may also result from cell overcharge.

The XPS analysis revealed that overcharge of the vanadium redox cell results in oxidation of the graphite-felt electrodes by the formation of various C–O functional groups (particularly –OH and C=O groups) so that, with increasing overcharge time, the concentration

Table 6
C 1s peak positions and relative peak area for overcharged and normal operation felt electrodes

Sample identification	Main Peak		Oxide 1		Oxide 2		Oxide 3	
	Position (eV)	Area (%)	Position (eV)	Area (%)	Position (eV)	Area (%)	Position (eV)	Area (%)
FMI, AC	284 5	81.3	285.9	13.0	287.6	2.2	288 9	3.3
FMI, OC1	284.5	71.2	285.9	15 2	286.7	7.4	288 9	5.2
GFD2, AC	284 5	85.5	285.9	11.2	287.7	1.7	289 0	1.6
GFD2, OC1	284 6	71.2	286.1	14.9	287.4	9.5	288 9	4.6

of higher oxidation-state groups increases on the surface. Compared with graphite-felt samples cycled normally in a vanadium redox cell, a large difference in the concentration of higher oxides, namely, C=O, COOH and COOR, is also observed with overcharge. This is confirmed by cyclic-voltammetric analysis of the graphite-felt electrodes. Furthermore, the XPS analysis also points to a loss in surface graphitization (aromaticity) with overcharge as the felt becomes oxidized.

The presence and concentration of different functional groups on the surface of the graphite-felt electrodes has been shown previously to affect the electrochemical behaviour of the electrodes and to lead to variations in cell efficiencies in the vanadium redox battery [24].

Further studies are currently being undertaken to understand better the role of the various functional groups on electrode performance and to determine what effect extended overcharge has on both short- and long-term electrode performance in the vanadium redox battery.

Acknowledgement

This work was funded by a grant from the Australia Research Council.

References

[1] Redox flow cell development and demonstration project, *NASA TM-79067*, US Department of Energy, 1979, p 31
[2] NASA redox storage system development project, Calendar year 1980, *DOE/NASA/12726-18, NASA TM-82940*, 1982, p. 19.
[3] NASA redox storage system development project, Calendar year 1981, *DOE/NASA/12726-19, NASA TM-83087*, 1983, p. 19
[4] NASA redox storage system development project, Calendar year 1980, *DOE/NASA/12726-23, NASA TM-83469*, 1983, p 4.
[5] K. Nozaki, H. Kaneko, M. Negishi and T. Ozawa, *Proc Symp. Advances in Battery Materials and Processes, Washington, DC, USA*, Proc. Vol. 84-4, The Electrochemical Society, Pennington, NJ, USA, 1984, p. 143
[6] K. Nozaki and T. Ozawa, *Proc. 17th Int Energy Conversion Engineering Conf, 1982*, p. 610.
[7] K. Nozaki, O. Hamamato, K. Mine and T Ozawa, *Denki Kagaku, 55* (1987) 229, in Japanese.
[8] P A. Thrower, *Proc Workshop Electrochemistry of Carbon, Cleveland, OH, USA, Aug 1983*, The Electrochemical Society, Pennington, NJ, USA, Proc. Vol. 84-5, p 40
[9] T.C Golden, R.G. Jenkins, Y. Otake and A.W. Scaroni, *Proc Workshop Electrochemistry of Carbon, Cleveland, OH, USA, Aug 1983*, The Electrochemical Society, Pennington, NJ, USA, Proc. Vol. 84-5, p. 61.
[10] L S Singer, *Proc Workshop Electrochemistry of Carbon, Cleveland, OH, USA, Aug. 1983*, The Electrochemical Society, Pennington, NJ, USA, Proc. Vol 84-5, p. 26.
[11] L.S. Singer and I.C. Lewis, *Appl. Spectrosc, 36* (1982) 52
[12] S Zhong, C Padeste, M. Kazacos and M Skyllas-Kazacos, *J Power Sources, 45* (1993) 29.
[13] S. Zhong, *Ph D Thesis*, University of NSW, Australia, 1992
[14] Y. Xie and P.M.A. Sherwood, *Chem Mater., 2* (1990) 293.
[15] Y. Xie and P M.A Sherwood, *Appl Spectrosc, 44* (1990) 797.
[16] Y. Xie and P.M.A. Sherwood, *Appl. Spectrosc, 43* (1989) 1153.
[17] Y Xie and P.M A. Sherwood, *Chem Mater., 1* (1989) 427
[18] C. Kozlowski and P.M.A. Sherwood, *J. Chem Soc, Faraday Trans. 1, 80* (1984) 2099.
[19] C. Kozlowski and P.M.A Sherwood, *J. Chem Soc, Faraday Trans 1, 81* (1985) 2745
[20] C. Kozlowski and P.M.A. Sherwood, *Carbon, 24* (1986) 357
[21] C Kozlowski and P.M.A. Sherwood, *Carbon, 25* (1987) 751
[22] A Proctor and P.M.A Sherwood, *J Electron Spectrosc Relat Phenom., 27* (1982) 39.
[23] A Proctor and P.M.A Sherwood, *Carbon, 21* (1983) 53
[24] B. Sun, *Ph D Thesis*, University of NSW, Australia, 1991